Appearance Reconstruction of Fluorescent Objects for Different Materials and Light Source

Shoji Tominaga, Keiji Kato, Keita Hirai, and Takahiko Horiuchi;
Graduate School of Engineering, Chiba University, Japan

Abstract

This paper proposes a method for reconstructing the scene appearance of fluorescent objects under different conditions of materials and light source. First, the observed spectral image of two fluorescent objects with the mutual illumination effect is described by the multiplication of the spectral functions and the geometric factors. Second, the observed image is decomposed into spectral component images by the ridge regression approach. Third, the geometric factor of the self-luminescent component is separated into the direct and indirect illumination components by taking the spatial distributions of reflection and interreflection into account. Then the scene appearance of the two fluorescent objects under different conditions is reconstructed using the five components of (1) reflection, (2) interreflection, (3) luminescence by direct illumination, (4) luminescence by indirect illumination, and (5) interreflection by fluorescent illumination. The feasibility is shown using two scenes consisting of two fluorescent objects.

Introduction

The appearance of three-dimensional objects in a scene is constructed based on such physical quantities as scene illuminant, object geometries, and object surface reflectances. Real scenes often exhibit significant mutual illumination between their surfaces, which must be accounted in the appearance construction process. The analysis of the mutual illumination of non-fluorescent objects was studied in the related fields such as color science, imaging technology, and computer vision [1]-[4], where the problem of appearance construction of the scene was seldom discussed. The study of the appearance of fluorescent objects had also been very limited, despite its importance in color imaging science and technology.

Appearance reconstruction of objects under different conditions of material properties and light source is always necessary in daily life settings. For instance, people want to control visual appearance and impression of the scene objects such as interior, outdoor objects, and clothing [5]-[6]. In previous studies, we proposed a multispectral imaging method to estimate the Donaldson matrix representing the bispectral characteristics of a fluorescent object [7]-[8]. By estimating the Donaldson matrix, appearance of the fluorescent object under different illuminants can be produced. We also analyzed the mutual illumination phenomenon between two different fluorescent objects [9]-[10]. We showed that the Donaldson matrices can be estimated from the observed spectral images even if the mutual illumination effect exists. However in the previous studies, the appearance reconstruction was available for only the case of change in illuminant.

The present paper discusses the appearance reconstruction of fluorescent objects with the mutual illumination effect, and it focuses on the extended problem of scene appearance reconstruction of the fluorescent objects influenced by the mutual illumination, under different illuminants by referring to different fluorescent material characteristics.

First, we model the observed spectral image of fluorescent objects with the mutual illumination effect. The observed image is described by the multiplication of the spectral functions depending on wavelength and the geometric factors depending on spatial location of the surfaces. Second, the appearance of the observed scene is decomposed into several components on spectral compositions, which are (1) diffuse reflection, (2) diffuse-diffuse interreflection, (3) fluorescent self-luminescence, and (4) interreflection caused by the fluorescent illumination from the adjacent surfaces. Note that the term of fluorescent interreflection is often numerically very small compared with the other components so that the standard least-squared estimator is too unstable to estimate the geometric factors. Since we cannot neglect the interreflection component, a ridge regression approach is applied to find a reliable solution for the component estimation problem.

We note that the fluorescent luminescence component consists of two different emission processes with the same emission spectrum. One emission is excited by direct illumination from light source, and another is excited by indirect illumination reflected from the other surfaces. A separation method is then devised to further decompose the self-luminescent term into the direct and indirect illumination components. The scene appearance of the target objects with the same geometric factors but different material characteristics under different illuminants is reconstructed based on the five component images of the original observed images. Each component image is constructed with the multiplication of the geometric factors and the spectral functions. We replace the terms of spectral functions with arbitrary Donaldson matrices and illuminant. Realistic appearances are then rendered as spectral images under the different conditions.

Observation Model of Fluorescent Objects with Mutual Illumination

The bispectral radiance factor of a fluorescent object is represented by a Donaldson matrix $D(\lambda_{em},\lambda_{ex})$ as a two-variable function of the excitation wavelength λ_{ex} and the emission/reflection wavelength λ_{em}. The diagonal at $\lambda_{em}=\lambda_{ex}$ represents the reflected radiance factor $D_{ref}(\lambda_{em},\lambda_{ex})$ consisting of surface-spectral reflectance $S(\lambda)$. The luminescent radiance factor $D_{lum}(\lambda_{em},\lambda_{ex})$ by fluorescent emission is located in the off-diagonal at $\lambda_{em}>\lambda_{ex}$, which can be separated into the excitation and emission wavelength components as $D_{lum}(\lambda_{em},\lambda_{ex})=\alpha(\lambda_{em})\beta(\lambda_{ex})$. The excitation spectrum is assumed to be normalized as $\int\beta(\lambda_{ex})d\lambda_{ex}=1$. A discrete form of the Donaldson matrix is represented in an $N\times N$ matrix as

$$\mathbf{D}=\mathbf{D}_{ref}+\mathbf{D}_{lum}$$
$$=\begin{bmatrix} s_1 & 0 & \cdots & 0 \\ 0 & s_2 & \ddots & \vdots \\ \vdots & \ddots & \ddots & 0 \\ 0 & \cdots & 0 & s_N \end{bmatrix}+\begin{bmatrix} 0 & & \cdots & & 0 \\ \alpha_2\beta_1 & 0 & & & \\ \alpha_3\beta_1 & \alpha_3\beta_2 & 0 & & \vdots \\ \vdots & \vdots & \ddots & \ddots & \\ \alpha_N\beta_1 & \alpha_N\beta_2 & \cdots & \alpha_N\beta_{N-1} & 0 \end{bmatrix}, \quad (1)$$

where the elements s_i (i = 1, 2, .., N) represent the reflected radiance factor, and the elements α_i (i = 2, 3, .., N), and β_i (i = 1, 2, .., N - 1) represent the emission spectrum and the excitation spectrum, respectively. The observation of a fluorescent object surface at location $\mathbf{x}$ = (x, y) can be described as a continuous function of wavelength

$$y(\mathbf{x},\lambda_{em})=f_{\text{ref}}(\mathbf{x})S(\lambda_{em})E(\lambda_{em})+f_{\text{lum}}(\mathbf{x})\alpha(\lambda_{em})\int_{350}^{\lambda_{em}}\beta(\lambda_{ex})E(\lambda_{ex})d\lambda_{ex} \quad (2)$$

Suppose that the two objects with different Donaldson matrices are located closely. These surfaces are matte and illuminated uniformly by a single illuminant $E(\lambda)$. The spectral radiances observed from the surfaces contain the mutual illumination. When we assume that the mutual illumination is based on only one reflection/emission between the two surfaces, the observations are represented as [9]

$$\begin{aligned} & y_i(\mathbf{x},\lambda_{em}) \\ & =f_{i1}(\mathbf{x})S_i(\lambda_{em})E(\lambda_{em})+f_{i2}(\mathbf{x})S_i(\lambda_{em})S_j(\lambda_{em})E(\lambda_{em}) \\ & +f_{i3}(\mathbf{x})\alpha_i(\lambda_{em})\int_{350}^{\lambda_{em}}\beta_i(\lambda_{ex})E(\lambda_{ex})d\lambda_{ex} \\ & +f_{i4}(\mathbf{x})\alpha_i(\lambda_{em})\int_{350}^{\lambda_{em}}\beta_i(\lambda_{ex})S_j(\lambda_{ex})E(\lambda_{ex})d\lambda_{ex} \\ & +f_{i5}(\mathbf{x})\alpha_i(\lambda_{em})\int_{350}^{\lambda_{em}}\beta_i(\lambda_{ex})\alpha_j(\lambda_{ex})\left(\int_{350}^{\lambda_{em}}\beta_j(\lambda'_{ex})E(\lambda'_{ex})d\lambda'_{ex}\right)d\lambda_{ex} \\ & +f_{i6}(\mathbf{x})S_i(\lambda_{em})\alpha_j(\lambda_{em})\int_{350}^{\lambda_{em}}\beta_j(\lambda_{ex})E(\lambda_{ex})d\lambda_{ex} \end{aligned} \quad (3)$$

where (i = 1, 2, j = 1, 2). We suppose that the excitation range starts from 350 nm [7]. Note that the weights $f_{ij}(\mathbf{x})$ for spectral functions are variable of location $\mathbf{x}$ and independent of wavelength λ, which are called the geometric factors in this paper.

The first and third terms in Eq.(3) represent the diffuse reflection and fluorescent emission on each surface by the direct illumination of the light source. The other terms include the mutual illumination effect. The second term represents interreflection between the diffuse reflections of both surfaces. Let us investigate the spectral compositions of the third to fifth terms. These spectral compositions are described as

$$\begin{aligned} & g_{i3}(\lambda_{em})=\alpha_i(\lambda_{em})c_{i3}(\lambda_{em}), \quad g_{i4}(\lambda_{em})=\alpha_i(\lambda_{em})c_{i4}(\lambda_{em}), \\ & g_{i5}(\lambda_{em})=\alpha_i(\lambda_{em})c_{i5}(\lambda_{em}), \end{aligned} \quad (4)$$

where (i = 1, 2, j = 1, 2),

$$\begin{aligned} c_{i3}(\lambda_{em}) &= \int_{350}^{\lambda_{em}}\beta_i(\lambda_{ex})E(\lambda_{ex})d\lambda_{ex}, \\ c_{i4}(\lambda_{em}) &= \int_{350}^{\lambda_{em}}\beta_i(\lambda_{ex})S_j(\lambda_{ex})E(\lambda_{ex})d\lambda_x, \\ c_{i5}(\lambda_{em}) &= \int_{350}^{\lambda_{em}}\beta_i(\lambda_{ex})\alpha_j(\lambda_{ex})\left(\int_{350}^{\lambda_{ex}}\beta_j(\lambda'_{ex})E(\lambda'_{ex})d\lambda'_{ex}\right)d\lambda_{ex}. \end{aligned} \quad (5)$$

The spectral functions g_{i3}, g_{i4}, and g_{i5} are the emission functions of $\alpha_i(\lambda)$ modified by the weights c_{i3}, c_{i4}, and c_{i5}. Figure 1 shows the spectral curves of the reflectance, the emission spectra, and the excitation spectra for two surfaces used in our experiment. Figure 2 depicts the spectral functions g_{i3}, g_{i4}, and g_{i5} computed using the spectral curves in Figure 1 under white illumination for Surfaces 1 and 2. We can see that the three spectral functions have essentially the same spectral composition as $\alpha_i(\lambda)$. We also note that g_{i5} is effective only if the emission of one surface is in the range of the excitation wavelength of the other surface. If the ranges disjoint, it disappears. Note in Figure 2 (b) that $g_{25}=0$.

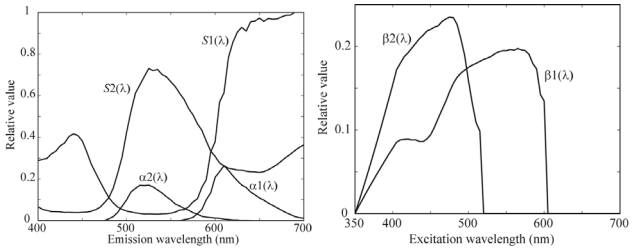

(a) Reflectances and emission spectra *(b) Excitation spectra*

Figure 1. *Spectral curves of the reflectances, the emission spectra, and the excitation spectra for two objects used in our experiment.*

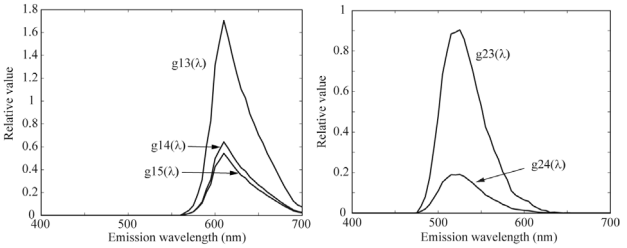

Figure 2. *Spectral functions g_{13} (g_{23}), g_{14} (g_{24}), and g_{15} (g_{25}) computed using the spectral curves in Figure 1 under white illumination for Surface 1 (Surface 2). Note $g_{25}=0$.*

When we summarize the different terms in Eq.(3) with the same spectral composition into one group, the above observation equations can be rewritten based on the spectral components as in the form:

$$\begin{aligned} y_i(\mathbf{x},\lambda_{em})=&F_{i1}(\mathbf{x})S_i(\lambda_{em})E(\lambda_{em})+F_{i2}(\mathbf{x})S_i(\lambda_{em})S_j(\lambda_{em})E(\lambda_{em}) \\ &+F_{i3}(\mathbf{x})C_{i1}(\lambda_{em})\alpha_i(\lambda_{em})+F_{i4}(\mathbf{x})C_{i2}(\lambda_{em})S_i(\lambda_{em})\alpha_j(\lambda_{em}) \end{aligned} \quad (6)$$

where (i = 1, 2, j = 1, 2),

$$C_{i1}(\lambda_{em}) = c_{i3}(\lambda_{em}) + c_{i4}(\lambda_{em}) + c_{i5}(\lambda_{em}),$$
$$C_{i2}(\lambda_{em}) = \int_{350}^{\lambda_{em}} \beta_j(\lambda_{ex}) E(\lambda_{ex}) d\lambda_{ex}. \quad (7)$$

It is important to note that the observed radiance factor on each surface consists of only four spectral components corresponding to (1) diffuse reflection, (2) diffuse-diffuse interreflection, (3) fluorescent self-luminescence, and (4) interreflection caused by the fluorescent illumination from the adjacent surface.

Appearance Decomposition Based on Spectral Compositions

We summarize the observation model in Eq.(6) into a matrix form. Let $\mathbf{s}_1$ (or $\mathbf{s}_2$) and $\boldsymbol{\alpha}_1$ ($\boldsymbol{\alpha}_2$) be N-dimensional column vectors representing the reflectance and emission spectra. Also, let be $\mathbf{c}_{ij}(i,j=1,2)$ N-dimensional column vectors representing the spectral functions $C_{ij}(\lambda)$ $(i,j=1,2)$. Using these symbols, let $\mathbf{A}_1$ ($\mathbf{A}_2$) be an N×4 matrix representing the spectral component functions and $\mathbf{F}_1(\mathbf{x})$($\mathbf{F}_2(\mathbf{x})$) be 4-dimensional column vectors representing the geometric factors as follows:

$$\begin{aligned}
\mathbf{A}_1 &= \left[\mathbf{s}_1 \cdot \mathbf{e} \quad \mathbf{s}_1 \cdot \mathbf{s}_2 \cdot \mathbf{e} \quad C_{11}\boldsymbol{\alpha}_1 \quad C_{12}\mathbf{s}_1 \cdot \boldsymbol{\alpha}_2\right], \\
\mathbf{A}_2 &= \left[\mathbf{s}_2 \cdot \mathbf{e} \quad \mathbf{s}_1 \cdot \mathbf{s}_2 \cdot \mathbf{e} \quad C_{21}\boldsymbol{\alpha}_2 \quad C_{22}\mathbf{s}_2 \cdot \boldsymbol{\alpha}_1\right] \\
\mathbf{F}_1(\mathbf{x}) &= \left[F_{11}(\mathbf{x}) \quad F_{12}(\mathbf{x}) \quad F_{13}(\mathbf{x}) \quad F_{14}(\mathbf{x})\right]^t, \\
\mathbf{F}_2(\mathbf{x}) &= \left[F_{21}(\mathbf{x}) \quad F_{22}(\mathbf{x}) \quad F_{23}(\mathbf{x}) \quad F_{24}(\mathbf{x})\right]^t
\end{aligned} \quad (8)$$

where symbols $\cdot$ and t represent element-wise multiplication and matrix transposition, respectively. Then the observations with mutual illumination effects are modeled in a simple matrix equation as

$$\mathbf{y}_1(\mathbf{x}) = \mathbf{A}_1\mathbf{F}_1(\mathbf{x}), \quad \mathbf{y}_2(\mathbf{x}) = \mathbf{A}_2\mathbf{F}_2(\mathbf{x}). \quad (9)$$

Since the matrices $\mathbf{A}_1$ ($\mathbf{A}_2$) are calculated from the Donaldson matrices, the spectral decomposition of scene appearance is reduced to solve a linear estimation problem in Eq.(9). If $\mathbf{A}_1^t\mathbf{A}_1$ ($\mathbf{A}_2^t\mathbf{A}_2$) are of full rank, the estimates of geometric factors $\mathbf{F}_1(\mathbf{x})$ ($\mathbf{F}_2(\mathbf{x})$) are determined at every pixel point $\mathbf{x}$ by using a standard method of linear least squares to minimize a residual error $\|\mathbf{y} - \mathbf{A}\mathbf{F}\|^2$, so that the observed spectral radiance image is decomposed into four spectral component images.

However, we often encounter that the matrices are close to rank deficient. For instance, the forth component $\mathbf{A}_i(4) = \mathbf{c}_{i2} \cdot \mathbf{s}_i \cdot \boldsymbol{\alpha}_j$ represents the interreflection caused by the fluorescent illumination from the adjacent surface, which is much smaller than the other components, so that $\mathbf{A}_i^t\mathbf{A}_i$ is close to singular and the estimates of $\mathbf{F}_1(\mathbf{x})$($\mathbf{F}_2(\mathbf{x})$) are unstable.

In this paper, a ridge regression approach is applied to get reliable estimates under such an ill condition [11]. We consider minimization of a new quantity $\|\mathbf{y} - \mathbf{A}\mathbf{F}\|^2 + \lambda\|\mathbf{F}\|^2$. Hence we minimize the quantity which is the sum of the squared residuals, plus a term proportional to the sum of the squared parameters of $\mathbf{F}$. The solution for the minimization is given as

$$\begin{aligned}
\hat{\mathbf{F}}_1 &= \left[\mathbf{A}_1^t\mathbf{A}_1 + \lambda\mathbf{I}\right]^{-1}\mathbf{A}_1^t\mathbf{y}_1 \\
\hat{\mathbf{F}}_2 &= \left[\mathbf{A}_2^t\mathbf{A}_2 + \lambda\mathbf{I}\right]^{-1}\mathbf{A}_2^t\mathbf{y}_2
\end{aligned}, \quad (10)$$

where λ is called the ridge parameter and $\mathbf{I}$ is an identity matrix. From a statistical point of view, the above new estimates are no longer unbiased, that is, their expected values are not equal to the true values. However, the variance of the above estimates can be smaller than that of the least-squares estimator, that is, so much reliable. The ridge parameter is determined based on the signal-to-noise ratio of the imaging system in this paper.

Estimation of Geometric Factors

The original observed image is decomposed into the four spectral components when the geometric factors $\mathbf{F}(\mathbf{x})$ are estimated using Eq.(10) every pixel point $\mathbf{x}$. The spectral decomposition does not necessarily correspond to the physical component decomposition of reflection and emission/excitation. Figure 3 shows a scene picture of the two fluorescent objects with the mutual illumination effect where a green cube is placed on a pink plane. The spectral curves of reflectance, emission spectra, and excitation for the two objects are shown in Figure 1. The observed spectral image is decomposed into the four component images. Figure 4 shows an image set of the geometric factors $F_1(\mathbf{x})$, $F_2(\mathbf{x})$, $F_3(\mathbf{x})$, $F_4(\mathbf{x})$. These geometric factor images reveal the location distributions where (1) diffuse reflection, (2) diffuse-diffuse interreflection, (3) self-luminescence, and (4) interreflection by fluorescence happen in the scene. The component of (3) self-luminescence is constructed with different physical process as discussed in the previous section. However, this component cannot be decomposed further on the basis of spectral composition.

The self-luminescent component is separated into two main fluorescent emission processes. One emission is excited by direct illumination from the light source, and another is excited by indirect illumination reflected from the other surface. We note that fluorescence emitted from any surface location on an object has non-directional characteristics, and is uniform to all directions. This property is similar to the Lambert matte surface where diffuse reflection occurs uniformly to all directions. The similarity between fluorescent emission and light reflection suggests that the two types of fluorescent emission by direct and indirect illuminations correspond to the diffuse reflection component and the diffuse-diffuse interreflection component. Therefore, the geometric factor of the self-luminescent component is decomposed into the direct and indirect illumination components by taking the two reflection types into account. The above consideration leads to a simple equation as follows:

$$F_3(\mathbf{x}) = d_1F_1(\mathbf{x}) + d_2F_2(\mathbf{x}), \quad (11)$$

where $F_1(\mathbf{x})$ and $F_2(\mathbf{x})$ are the geometric factors of the diffuse reflection and the diffuse-diffuse interreflection. The parameters d_1 and d_2 are the weighting coefficients, which are determined to minimize the fitting error over the entire image. We have d_1 = 0.87 and d_2 = 0.01 for the geometric factor images in Figure 4.

Thus the self-luminescent term can be decomposed into two emission components with different local distributions.

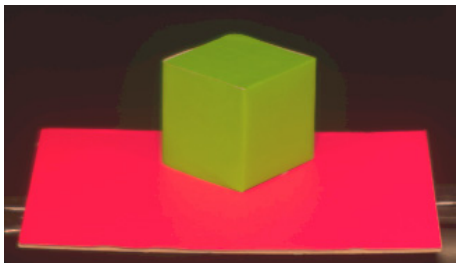

Figure 3. *Scene picture of two fluorescent objects with the mutual illumination effect. The spectral function curves for the two objects are shown in Figure 1.*

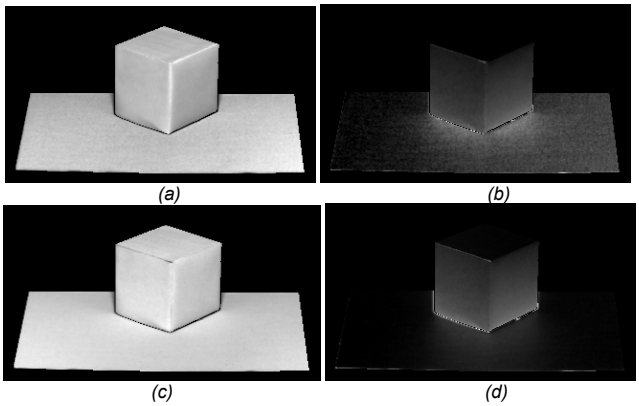

Figure 4. *Image set of the geometric factors* $F_1(\mathbf{x}), F_2(\mathbf{x}), F_3(\mathbf{x}), F_4(\mathbf{x})$ *. (a)* $F_1(\mathbf{x})$ *for diffuse reflection, (b)* $F_2(\mathbf{x})$ *for diffuse-diffuse interreflection, (c)* $F_3(\mathbf{x})$ *for self-luminescence, and (d)* $F_4(\mathbf{x})$ *for interreflection by fluorescence.* The value for the ridge parameter is 0.04.

Appearance Reconstruction

Let us consider reconstruction of the scene appearance for different conditions of materials and light source. The geometric factors obtained from the observed image of two fluorescent objects retain the important scene information such as shape information, shading information, and surface roughness, except for the spectral information such as material's Donaldson matrix and illuminant. Therefore, we can reconstruct the scene appearance for different materials and light source on the basis of the same geometric factors.

The spectral radiances observed from the scene of two adjacent fluorescent objects are constructed with five physical components of (1) reflection, (2) interreflection, (3) luminescence excited by direct illumination, (4) luminescence excited by indirect illumination, and (5) interreflection by fluorescent illumination. The spectral functions and the geometric factors belonging to the respective components are rewritten as follows:

$$\begin{aligned}\mathbf{A}_1^{'} &= \left[\mathbf{s}_1\cdot\mathbf{e} \quad \mathbf{s}_1\cdot\mathbf{s}_2\cdot\mathbf{e} \quad \mathbf{c}_{11}\cdot\boldsymbol{\alpha}_1 \quad \mathbf{c}_{12}\cdot\boldsymbol{\alpha}_1 \quad \mathbf{c}_{13}\cdot\mathbf{s}_1\cdot\boldsymbol{\alpha}_2\right],\\ \mathbf{A}_2^{'} &= \left[\mathbf{s}_2\cdot\mathbf{e} \quad \mathbf{s}_1\cdot\mathbf{s}_2\cdot\mathbf{e} \quad \mathbf{c}_{21}\cdot\boldsymbol{\alpha}_2 \quad \mathbf{c}_{22}\cdot\boldsymbol{\alpha}_2 \quad \mathbf{c}_{23}\cdot\mathbf{s}_2\cdot\boldsymbol{\alpha}_1\right],\end{aligned} \quad , \quad (12)$$

$$\begin{aligned}\mathbf{F}_1^{'}(\mathbf{x}) &= \left[F_{11}^{'}(\mathbf{x}) \quad F_{12}^{'}(\mathbf{x}) \quad F_{13}^{'}(\mathbf{x}) \quad F_{14}^{'}(\mathbf{x}) \quad F_{15}^{'}(\mathbf{x})\right]^t,\\ \mathbf{F}_2^{'}(\mathbf{x}) &= \left[F_{21}^{'}(\mathbf{x}) \quad F_{22}^{'}(\mathbf{x}) \quad F_{23}^{'}(\mathbf{x}) \quad F_{24}^{'}(\mathbf{x}) \quad F_{25}^{'}(\mathbf{x})\right]^t,\end{aligned} \quad , \quad (13)$$

where the vectors $\mathbf{c}_{i1}$, $\mathbf{c}_{i2}$, and $\mathbf{c}_{i3}$ are calculated using $c_{i3}(\lambda)$, ($c_{i4}(\lambda)$ + $c_{i5}(\lambda)$) in Eq.(5), and $C_{i2}(\lambda)$ in Eq.(7), respectively. It is noted that the geometric factors for the self-luminescence are determined by the linear fitting of the reflection vector and the interreflection vector to the total self-luminescent factor, which result in

$$\begin{aligned}F_{13}^{'}(\mathbf{x}) &= d_{11}F_{11}^{'}(\mathbf{x}), \quad F_{14}^{'}(\mathbf{x}) = d_{12}F_{12}^{'}(\mathbf{x}),\\ F_{23}^{'}(\mathbf{x}) &= d_{21}F_{21}^{'}(\mathbf{x}), \quad F_{24}^{'}(\mathbf{x}) = d_{22}F_{22}^{'}(\mathbf{x}).\end{aligned} \quad , \quad (14)$$

Figure 5 shows the flow for the appearance reconstruction. The factors $\mathbf{F}_1^{'}(\mathbf{x})$ and $\mathbf{F}_2^{'}(\mathbf{x})$ are spatially disjoint. The combinations ($\mathbf{F}_1^{'}(\mathbf{x})$, $\mathbf{F}_2^{'}(\mathbf{x})$) cover the entire object surfaces, which represent the spatially local distributions of the respective geometric factors. Any pair of materials can be used for appearance reconstruction. The scene appearance is constructed in the range [400, 700 nm], which is sampled in equal intervals of 5 nm. Then the dimension of spectral functions is N = 61. The excitation vector has N = 71 with starting from 350 nm. The illuminant spectral-power distribution is specified in the range [350, 700 nm].

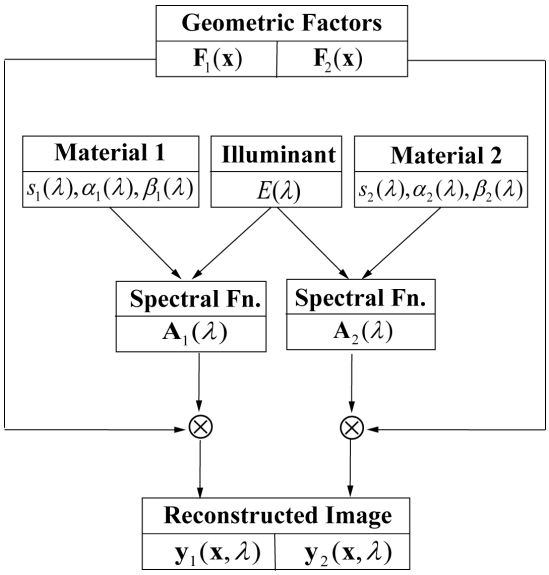

Figure 5. *Flow for reconstructing the scene appearance for different conditions of materials and illuminant.*

The spectral radiances of object scene for the desired materials and illuminant are calculated pixel-by-pixel by combining the five spectral components as

$$\mathbf{y}_1^{'}(\mathbf{x}) = \mathbf{A}_1^{'}\mathbf{F}_1^{'}(\mathbf{x}), \quad \mathbf{y}_2^{'}(\mathbf{x}) = \mathbf{A}_2^{'}\mathbf{F}_2^{'}(\mathbf{x}) . \quad (15)$$

We note here that the first two components $\mathbf{A}_1^{'}(1)$, $\mathbf{A}_1^{'}(2)$ ($\mathbf{A}_2^{'}(1)$, $\mathbf{A}_2^{'}(2)$) spectrally depend on illuminant, and the remaining

three components are illuminant independent but dependent on emission spectra. The above 61-dimensinal radiance vectors are finally converted into a display color space where a color image of the reconstructed appearance is rendered.

Experimental Results

We used the scene of two fluorescent objects shown in Figure 3. The objects were illuminated with an incandescent lamp at an incidence angle of 45 degrees from the front. The spectral image was captured at 5 nm intervals in the range [400, 700 nm] by using an imaging system consisting of a monochrome CCD camera and a LCT filter. The Donaldson matrix of each fluorescent object was obtained separately by the two illuminant projection method [7]. Figure 1 showed the spectral curves of the reflectances, the emission spectra, and the excitation spectra, where the numbers 1 and 2 indicate the pink plane and the green cube, respectively.

The estimated geometric factors were shown in the image set of Figure 4 for (a) the reflection, (b) the interreflection, (c) the self-luminescence, and (d) the interreflection by fluorescence. The ridge parameter was set to $\lambda = 0.04$. The geometric factor for the self-luminescence was further decomposed into the direct and indirect illumination components.

A different set of fluorescent materials and illuminant was used to examine the feasibility of the proposed method for appearance reconstruction. We exchanged the original Donaldson matrices of the two objects so that the plane has the green material with ($S_2(\lambda), \alpha_2(\lambda), \beta_2(\lambda)$) and the cube has the pink material with ($S_1(\lambda), \alpha_1(\lambda), \beta_1(\lambda)$) in Figure 1. We assumed the illuminant to be an artificial sunlight. The scene appearance of the same geometries was reconstructed with the different conditions along the flow in Figure 5. Figure 6 demonstrates the color image set of the five spectral image components produced in the reconstruction process, where all images are displayed with the gamma correction of 2.3.

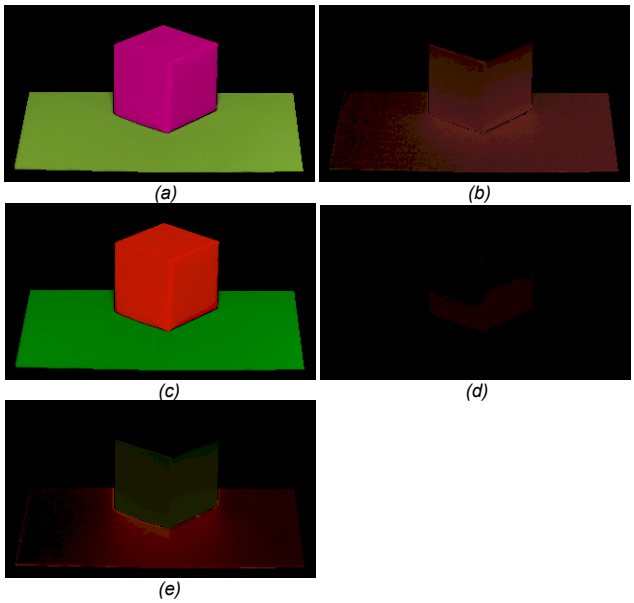

Figure 6. *Color image set of the five spectral image components. (a) Diffuse reflection, (b) diffuse-diffuse interreflection, (c) self-luminescence by direct illumination, (d) self-luminescence by indirect illumination, and (e) interreflection by fluorescence.*

We notice the following features for the respective components: (a) The first color image is constructed by object colors only. (b) The second is constructed with mixture of two object color by the interreflection, which is stronger around the boundary between the two objects. (c) The third is constructed with only fluorescent colors, which are uniform over the entire object surfaces because of uniform illumination. (d) The fourth is also constructed with only fluorescent colors, which, however, is a weak contribution limited to the surrounding of the boundary because of the indirect illumination. (e) The appearance of the fifth color image is constructed by the exchanged fluorescent colors around the boundary area between the two surfaces, as a result of the interreflection between the two fluorescence objects.

Figure 7 (a) shows a color image of the reconstructed scene appearance by linearly combining the above five component images. We constructed the actual target scene, where two objects were made of the same fluorescent materials of the same sizes. The pink cube placed on the green plane was illuminated with a real lamp of artificial sunlight at the same incidence angle. Figure 7 (b) shows a color image of the real scene. We calculated the color difference between the reconstructed image and the original image. The average values of ΔE_{ab} are 11.7 for the green object and 10.9 for the pink object. A side-by-side comparison in Figure 7 suggests that the appearance of the reconstructed image is close to the real appearance.

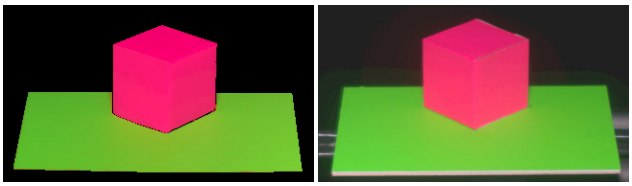

Figure 7. *Appearance comparison between the reconstructed scene and the real scene. (a) A color image of the reconstructed scene appearance by combining the five component images and (b) a color image of the real scene constructed using two real fluorescent materials and illuminant.*

Conclusions

We have proposed a method for reconstructing the scene appearance of fluorescent objects under different conditions of fluorescent materials and light source. First, the observed spectral image of two fluorescent objects with the mutual illumination effect was described by the multiplication of (1) spectral functions depending on wavelength and (2) the geometric factors depending on spatial location. Second, the appearance of the observed scene was decomposed on spectral properties. The ridge regression approach was applied to the observed image to estimate the reliable spectral image components of (1) diffuse reflection, (2) diffuse-diffuse interreflection, (3) fluorescent self-luminescence, and (4) interreflection caused by the fluorescent illumination. Third, the geometric factor of the self-luminescent component was separated into the direct and indirect illumination components by taking the spatial distributions of reflection and interreflection into account. The scene appearance of two fluorescent objects under different conditions was reconstructed using the five components of (1) reflection, (2) interreflection, (3) luminescence by direct

illumination, (4) luminescence by indirect illumination, and (5) interreflection by fluorescent illumination. In experiments, the feasibility of the proposed method was shown using two scenes consisting of two fluorescent objects with mutual illumination effect. The spectral image was captured from the first scene under the incandescent light, and decomposed into the five components to extract the geometric factors. The appearance of the second scene was reconstructed on the basis of the geometric factors obtained from the first scene. The predicted appearance was shown to be close to the real appearance.

Acknowledgments

This work was supported by JSPS KAKENHI Grant Number JP15H05926 (Grant-in-Aid for Scientific Research on Innovative Areas "Innovative SHITSUKAN Science and Technology").

References

[1] J. J. Koenderink and A. J. van Doorn, Geometrical modes as a general method to treat diffuse interreflections in radiometry, J. Optical Society of America, 73, 843-850 (1983).

[2] M.S. Drew and B.V. Funt, Variational approach to interreflection in color images, J. Optical Society of America A, 9, 1255-1265 (1992).

[3] S. Tominaga, Separation of reflection components from a color image, Proc. CIC5, 254-257 (1997).

[4] M. Langer, Model of how interreflections can affect color appearance, Color Res. Appl., Supplement 26, s218-s221 (2001).

[5] B. M. Oh, M. Chen, J. Dorsey, and F. Durand, Image-based modeling and photo editing, Proc. ACM SIGGRAPH, 433-442 (2001).

[6] S. Zelinka, H. Faung, M. Garland, and J. C. Hart, Interactive material replacement in photographs, Proc. Graphics Interface, 227-232 (2005).

[7] S. Tominaga, K. Hirai, and T. Horiuchi, Estimation of bispectral Donaldson matrices of fluorescent objects by using two illuminant projections, J. Optical Society of America A, 32, 1068- 1078 (2015).

[8] S. Tominaga, K. Kato, K. Hirai, and T. Horiuchi, Spectral image analysis and appearance reconstruction of fluorescent objects under different illuminations, Proc. 4th CIE Expert Symposium on Colour and Visual Appearance, 140-146 (2016).

[9] S. Tominaga, K. Kato, K. Hirai, and T. Horiuchi, Spectral image analysis of mutual illumination between florescent objects, J. Optical Society of America A, 33, 1476-1487 (2016).

[10] S. Tominaga, K. Kato, K. Hirai, and T. Horiuchi, Spectral image analysis of florescent objects with mutual illumination, Proc. CIC24, 59-64 (2016).

[11] W.N. van Wieringen, Lecture Note on Ridge Regression, arXiv: 1509.09169 (2015).

Author Biography

Shoji Tominaga received the Ph.D. degree in electrical engineering from Osaka University, Japan, 1975. In 2006, he joined Chiba University, where he was a Professor (2006-2013) and Dean (2011-2013) at Graduate School of Advanced Integration Science. He is now a Specially Appointed Researcher, Chiba University. He is also an Adjunct Professor, NTNU, Norway. His research interests include digital color imaging, multispectral imaging, and material appearance. He is a Fellow of IEEE, IS&T, SPIE, and OSA.